PUBLICATIONS

Online: ISSN 2008-949X

# **Journal of Mathematics and Computer Science**



Journal Homepage: www.isr-publications.com/jmcs

# A prey-predator approach to tumor-immune and cancer treatment: a circuit-based analysis with non-local derivatives



Chandrali Baishya<sup>a</sup>, Reny George<sup>b,\*</sup>, R. N. Premakumari<sup>c</sup>, Asharani J. Rangappa<sup>a</sup>, Sina Etemad<sup>d,e,f</sup>, Adnan Taan Alkhafaji<sup>g</sup>

#### **Abstract**

The dynamic interplay between the tumor and the immune system determines if cancer advances or retreats. This study investigates a three-dimensional nonlinear differential system incorporating tumor cells, hunting CTLs, and resting CTLs under the Caputo-Fabrizio fractional derivative framework. The complex and dynamic interaction between immune cells and tumor cells plays a crucial role in the development, progression, and treatment of cancer. Key dynamical aspects, such as the existence and uniqueness of solutions, equilibrium points, and their stability, are rigorously analyzed. To bridge theory with practical validation, circuit implementations are developed using MATLAB, enabling the comparison of computational precision and authenticity for the tumor model. This innovative approach highlights how circuit-based representations can enhance the understanding of tumor-immune dynamics, which further helps in the treatment of cancer. Numerical simulations, incorporating estimated parameter values, validate the theoretical findings and provide deeper insights into the system's behavior. These results contribute to a more comprehensive understanding of tumor progression and immune response modulation, paving the way for improved strategies in cancer treatment.

**Keywords:** Tumor-immune dynamics, Caputo-Fabrizio fractional derivative, circuit implementation, stability analysis, treatment of cancer.

2020 MSC: 26A33, 34A12, 34D20, 47N70.

©2026 All rights reserved.

#### 1. Introduction

Cancer, a non-communicable disease, has emerged as the most deadly and complex illness in the

Email addresses: baishyachandrali@gmail.com (Chandrali Baishya), renygeorge02@yahoo.com (Reny George), premakumarirn12@gmail.com (R. N. Premakumari), jrashudini@gmail.com (Asharani J. Rangappa), sina.etemad@gmail.com (Sina Etemad), taananhar@alayen.edu.iq (Adnan Taan Alkhafaji)

doi: 10.22436/jmcs.041.01.07

Received: 2025-05-06 Revised: 2025-06-12 Accepted: 2025-07-24

<sup>&</sup>lt;sup>a</sup>Department of Studies and Research in Mathematics, Tumkur University, Tumkur-572103, Karnataka, India.

<sup>&</sup>lt;sup>b</sup>Department of Mathematics, College of Science and Humanities in Al-Kharj, Prince Sattam bin Abdulaziz University, Al-Kharj 11942, Saudi Arabia.

<sup>&</sup>lt;sup>c</sup>Department of Mathematics, M.E.S. Degree College of Arts, Commerce and Science, Malleswaram, Bangalore 560003, Karnataka, India.

<sup>&</sup>lt;sup>d</sup>Department of Mathematics, Saveetha School of Engineering, Saveetha Institute of Medical and Technical Sciences, Saveetha University, Chennai 602 105, Tamil Nadu, India.

<sup>&</sup>lt;sup>e</sup>Department of Mathematics, Azarbaijan Shahid Madani University, Tabriz, Iran.

<sup>&</sup>lt;sup>f</sup>Mathematics in Applied Sciences and Engineering Research Group, Scientific Research Center, Al-Ayen University, Nasiriyah 64001, Irad.

<sup>&</sup>lt;sup>g</sup>Cardiology Department, College of Medicine, Al-Ayen University, Thi-Qar, Iraq.

<sup>\*</sup>Corresponding author

world. This disease is brought on by the body's aberrant or mutant cells proliferating out of control, and tumor cells are notorious for their capacity to multiply, divide, and expand rapidly [11, 13]. The main factors contributing to the growth of tumors are their ongoing multiplication and propensity for metastasis [19]. According to the American Cancer Society, there will be 609,820 cancer-related deaths and 1,958,310 new cases in the US in 2023. Between 2014 and 2019, there were 99,000 new instances of prostate cancer, representing an annual growth of 3%. Conversely, men seem to have more favorable incidence patterns. While melanoma, breast, uterine, and liver cancers increased, women's lung cancer decreased half as quickly as men's. The cancer death rate continued to decline despite the epidemic, saving 3.8 million lives and representing a 33% drop since 1991. However, the rising incidence of breast, prostate, and uterine corpus cancers, which cause the largest racial mortality disparities[34], may pose a challenge to future progress. After cardiovascular diseases, it is the second most deadly infection [30]. A wide range of illnesses, including over 200 conditions [1], fall under the general term "cancer" since they all involve aberrant cells with disrupted regular mechanisms that govern normal cellular division, growth, and death. Numerous genetic and metabolic processes tightly regulate and control the development, division, and death of normal cells. Cells develop abnormally when these pathways are disrupted for various reasons. Our immune system assists the host in the battle against harmful microorganisms and malignant cells. It is a complicated network of cells, cytokines, lymphoid tissues, and organs. In cancer development and progression, the immune system plays a dual role: it promotes tumor advancement through immunized host selection and suppresses tumor growth by destroying tumor cells or preventing expansion [33]. The processes of elimination, balance, and escape are involved in cancer immunoediting. Tumor growth is inhibited by elimination, cell expansion is regulated by equilibrium, and cancer cell variants with lower immunogenicity can proliferate into malignancies through escape [32, 37].

Mathematical modeling is an effective instrument that provides both quantitative and qualitative visualizations of important biological scenarios. An effective mathematical model can assist in better understanding the dynamic interplay between tumor cells and the immune system, which could be important in understanding the tumor and developing novel therapies for it. However, it is nearly impossible to develop mathematical models that accurately describe such complex interaction processes. The truth is that the complex relationship between immune components and malignant cells is represented by highly idealized mathematical models. Consequently, it's critical to develop basic mathematical models that can illustrate the majority of significant immunological occurrences. Several studies employed the idea of prey-predator to investigate the relationship between immune cells and tumors [12, 16, 17]. The preypredator model of the tumor-immune system differs from the conventional prey-predator framework. In the latter case, the survival of the immune population is not dependent on the amount of prey (tumor cells). Immune cells are the predators, and tumor cells are the prey. On their cell surface, tumor cells create specific antigens that are recognized and eliminated by the host's cellular immune response. For instance, a delay-induced model was used in [5] to examine the relationship between the tumor and the immune system as well as the control of the growth of malignant tumors. An analysis of the qualitative behavior of tumor-CD4+-cytokine interaction systems with therapies was conducted in [3]. A unique mathematical model for immune surveillance of malignancies has been created in [23]. Jordao and Tavares originate a comparative model encompassing both cancer cells and healthy cells, offering a comprehensive analysis of the suggested cancer model [15]. Khajanchi and Nieto explored the impact of time delay on the dynamics of the tumor system [18]. Additionally, Mahlbacher et al. contributed to a deeper understanding of the relationship between cancers and the immune system, developing a model crucial for informing cancer treatment strategies [24]. Idrees and Sohail have formulated a mathematical model based on experimental research, elucidating the interplay between tumor cells and cytotoxic T lymphocytes. For the past three centuries, only mathematicians, physicists, and engineers have utilized fractional calculus. However, fractional operations and their applicability have received a lot of attention recently in a lot of unusual fields, such as hydrology, signal processing, heat diffusion models, competing species, biology, [25, 27], medicine, finance, physics, synchronization of chaotic systems, atmospheric ocean problems, and hydrology [28, 29, 36, 38, 39]. Two integer order systems, which have been investigated using

fractional calculus, provide an explanation for the fluctuations of the tumor-immune system [35]. The paper [9] examines a fractional-order system that postulates tumor growth following drug application. For the tumor-immune system with treatments, a delay model with fractional order has been created in [31]. In [2], a mathematical model of immune response with cell-mediated tumor phenotypic heterogeneity has been studied. The authors of [10] provided a fractional derivative model that took radiation, cell reproduction, and cell repair into account.

In this work, a mathematical model of uncontrolled tumor regression and progression in immune system resistance is presented and analyzed, showing complex dynamic behavior in the parameter range of interest. In this paper, we review a mathematical model of cancer remission that was initially shown by Kaur and Ahmad [17]. Moving in line with the Sustainable Development Goal-3 of the United Nations, our primary contribution in this paper is the analysis of the tumor model using the Caputo-Fabrizio fractional derivative. A novel aspect of this work is the circuit-based implementation of the Simulink model in MATLAB to simulate the tumor dynamics. The study explores key theoretical components, including the conditions for the existence and uniqueness of solutions, as well as the local stability of equilibrium points. A significant contribution is the incorporation of threshold dynamics and the biological meanings of the stability of the equilibrium points are thoroughly justified.

The remainder of the paper is structured as follows. The fundamental definitions of the Caputo-Fabrizio fractional derivative are covered in Section 2. The model construction and description are discussed in Section 3, and the existence and uniqueness of the solution are analyzed in Section 4. Section 5 is dedicated to the circuit implementation. In Section 6, the dynamics of the system, such as equilibria and their local stability, and the validations of various threshold parameters are performed. The theoretical results are validated by using Adams-Bashforth numerical technique in Section 7. The overall work is concluded in Section 8.

#### 2. Preliminaries

Here we present certain results associated with the Caputo-Fabrizio fractional derivatives, which are utilized in this study to validate the conceptual results. As usual, the symbol  $L^2(\mathfrak{a},\mathfrak{b})$  introduces the space of square integrable functions on  $(\mathfrak{a},\mathfrak{b})$  and  $V[\mathfrak{a},\mathfrak{b}]$  introduces the collection of vector functions that operating on  $H^1(\mathfrak{a},\mathfrak{b})$  so that

$$H^1(\mathfrak{a},\mathfrak{b})=\left\{g:g\in L^2(\mathfrak{a},\mathfrak{b}),\ g^{'}\in L^2(\mathfrak{a},\mathfrak{b})\right\}.$$

Moreover,  $||W(t)|| = \sum_{i=1}^{3} \sup |w_i(t)|$  is the norm of  $W(t) = (w_1, w_2, w_3) \in [a, b]$ , and the supremum is taken on  $t \in [a, b]$ .

**Definition 2.1** ([26]). Let h(t) be a n-times continuously differentiable function and  $h^{(n)}(t)$  be integrable on  $[t_0,T]$ . The definition of the Caputo fractional derivative of order  $\alpha$  for a function h(t) is then given by

$${}^{C}D^{\alpha}h(t) = \frac{1}{\Gamma(1-\alpha)} \int_{t_0}^{t} \frac{h'(\zeta)}{(t-\zeta)^{\alpha}} d\zeta, \tag{2.1}$$

where  $h \in H^1(\mathfrak{a},\mathfrak{b})$  such that  $0 < \alpha < 1$ . The singularity occurs when  $t = \zeta$  for the kernel  $(t - \zeta)^{-\alpha}$  in (2.1). The following fractional derivative with exponential kernel was defined by Caputo and Fabrizio [6] in 2015 by varying the kernel  $(t - \zeta)^{-\alpha}$  with the function  $\exp(-\frac{\alpha(t - \zeta)}{1 - \alpha})$  and  $\frac{1}{\Gamma(1 - \alpha)}$  with  $\frac{A(\alpha)}{1 - \alpha}$ , that is

$$^{CF}D^{\alpha}h(t) = \frac{A(\alpha)}{1-\alpha} \int_{\alpha}^{t} \exp\left(-\frac{\alpha}{1-\alpha}(t-\zeta)\right) f^{'}(\zeta)d\zeta,$$

where  $A(\alpha)$  is any smooth positive function such that A(0) = A(1) = 1. The kernel does not exhibit singularity for  $t = \zeta$  in accordance with the Caputo-Fabrizio fractional derivative (CFFD), which states

that the derivative of a constant is zero. Afterwards, Losada and Nieto [22] constructed a new CFFD of order  $0<\alpha<1$  by altering the kernel  $(t-\zeta)^{-\alpha}$  with the function  $\exp(-\frac{\alpha(t-\zeta)}{1-\alpha})$  and  $\frac{1}{\Gamma(1-\alpha)}$  with  $\frac{1}{\sqrt{2\pi(1-\alpha^2)}}$  in (2.1), that is

$${^{CF}D}^{\alpha}f(t) = \frac{(2-\alpha)A(\alpha)}{2(1-\alpha)}\int_{0}^{t} exp\left(-\frac{\alpha}{1-\alpha}(t-\zeta)\right)f^{'}(\zeta)d\zeta.$$

**Definition 2.2.** Applying the mentioned method in [22], we can express the Caputo-Fabrizio fractional integral operator as follows:

$$^{CF}I_{t}^{\alpha}f(t)=\frac{2(1-\alpha)}{(2-\alpha)A(\alpha)}f(t)+\frac{2\alpha}{(2-\alpha)A(\alpha)}\int_{0}^{t}f(\zeta)d\zeta\text{, }t\geqslant0.$$

As per the definition given above, for order  $0 < \alpha < 1$ , the fractional integral of Caputo type can be obtained as the average of the function f and its integral of order one. This result follows that

$$\frac{2(1-\alpha)}{(2-\alpha)A(\alpha)} + \frac{2\alpha}{(2-\alpha)A(\alpha)} = 1.$$

The formula obtained from the earlier expression is as follows:

$$A(\alpha) = \frac{2}{2-\alpha}, \ 0 < \alpha < 1.$$

**Definition 2.3** ([22]). Consider the Caputo-Fabrizio type fractional initial value problem given by

$$^{CF}D_t^{\alpha}y(t) = f(t, y(t)), \quad 0 < \alpha \le 1, \quad y(0) = y_0,$$
 (2.2)

where  ${}^{CF}D_t^{\alpha}$  is a CFFD of order  $\alpha$ , and f is a continuous function. The equivalent Volterra-type integral form of the problem is formulated by

$$y(t) = y_0 + (1-\alpha) \int_0^t f(\tau, y(\tau)) \, d\tau + \alpha \int_0^t exp\left(-\frac{\alpha}{1-\alpha}(t-\tau)\right) f(\tau, y(\tau)) \, d\tau.$$

We define the Picard operator T on a suitable Banach space C[0,T] as

$$(\Im y)(t) = y_0 + (1-\alpha) \int_0^t f(\tau, y(\tau)) d\tau + \alpha \int_0^t \exp\left(-\frac{\alpha}{1-\alpha}(t-\tau)\right) f(\tau, y(\tau)) d\tau.$$

A function  $y \in C[0,T]$  is a solution of the Caputo-Fabrizio initial value problem (2.2) if and only if it is a fixed point of T, i.e., Ty = y.

**Lemma 2.4** ([26]). Let (X,d) be a complete metric space, and suppose the operator  $\mathfrak{T}:X\to X$  satisfies the contraction condition  $d(\mathfrak{T}x,\mathfrak{T}y)\leqslant k\,d(x,y),\,\forall x,y\in X$ , for some constant 0< k<1. Then  $\mathfrak{T}$  has a unique fixed point  $x^*\in X$ , and the sequence defined by the Picard iteration  $x_{n+1}=\mathfrak{T}x_n$  converges to  $x^*$ . In the context of fractional differential equations, if f(t,y) satisfies a Lipschitz condition in y, then the Picard operator  $\mathfrak{T}$  is a contraction on C[0,T], and hence, the Banach fixed point theorem guarantees the existence and uniqueness of the solution.

**Lemma 2.5** ([21]). Consider the system  ${}^{CF}D^{\alpha}_{\mathfrak{t}_{\mathfrak{o}}}x(\mathfrak{t})=f(\mathfrak{t},x),\ \mathfrak{t}>\mathfrak{t}_{\mathfrak{o}}.$  Let  $x(\mathfrak{t}_{0})$  be the starting condition, with  $0<\alpha\leqslant 1$  and  $h:[\mathfrak{t}_{0},\infty)\times\mho\to\mathbb{R}^{n},\mho\in\mathbb{R}^{n}.$  On  $[\mathfrak{t}_{0},\infty)\times\mho$ , the system has a unique solution if  $f(\mathfrak{t},x)$  admits the local Lipschitz criteria with respect to x.

#### 3. Mathematical model

We consider a system of three nonlinear differential equations with state variables: the density of tumor populations, the density of hunting CTLs, and the density of resting CTLs in a single tumorsite compartment at any given time t. With fractional-order derivatives, our model is an adaptation of the original model by Kaur and Ahmad [17]. The immune system's response is viewed by most mathematical models of the tumor-immune system as a single population of cells known as effector cells [7, 14, 20, 30], which are in charge of eradicating malignant cells. The dynamics of the immune system can be made more straightforward by this simplifying basis. The immune system kills tumor cells in two stages: hunting CTLs and resting CTLs. Tumor cells cannot be destroyed by resting CTLs, but they can be killed by hunting cells. Tumor cells are recognized and eliminated by the host's cellular immune system because of specific antigens they release on their surface. The cellular response of the immune system is executed by T cells. Antigen fragments on the surface of tumor cells are detected by specialized antibody-like receptors on the surface of developing T lymphocytes. Cell membrane proteins called Major Histocompatibility Complex (MHC) molecules bind antigens, which are the only antigens that T cells can recognize in most circumstances. The ability of resting T lymphocytes to distinguish between self and nonself is based on their recognition of the protein-based MHC molecule. Resting T lymphocytes can engulf tumor cells and release a range of growth factors called cytokines, but they are not able to eradicate the tumor cells. The cytotoxic T cells, also referred to as hunting cells, are triggered by chemical messenger switches called cytokines. In contrast to latent T cells, cytotoxic T lymphocytes usually release a high quantity of cytokines, along with lysergic causing damage to the target tumor cell. Taking into account the previously stated biological mechanism, we altered a mathematical model of immune response-related tumor formation. The following hypotheses are made by the model.

- In the absence of hunting CTLs, tumour cell growth is logistic.
- According to the law of mass action, the rate of elimination of tumor and hunting CTLs is proportional to their relative densities.
- The transition from resting to hunting cells occurs when the hunting cells directly contact the resting cells or when they come into contact with a chemical that spreads quickly (cytokines).
- In the absence of tumour cells, resting cells similarly follow logistic growth.
- The existence of tumor cells activates the resting cells, and this effect is mediated by the function of Michaelis-Menten.

Let X(t) represent the concentration of tumor cells in the given physiological space at time t, Y(t) represent the concentration of hunting CTLs, and Z(t) represent the concentration of resting CTLs. The model governing the interaction between X(t), Y(t), Z(t) is represented by the set of equations below:

$$\begin{split} \frac{dX}{d\tau} &= \alpha_1 X \left( 1 - \frac{X}{\alpha_2} \right) - \alpha_3 XY, \\ \frac{dY}{d\tau} &= \alpha_4 Y Z - \alpha_5 Y - \alpha_6 XY, \\ \frac{dZ}{d\tau} &= \alpha_7 Z \left( 1 - \frac{Z}{\alpha_8} \right) - \alpha_9 Y Z - \alpha_{10} Z + \frac{\alpha_{11} X Z}{X + \alpha_{12}}, \end{split}$$

$$(3.1)$$

where the intrinsic growth rate and carrying capacity of tumor cells are denoted, respectively, by  $a_1$  and  $a_2$ .  $a_3$  represents the rate at which hunting cells destroy tumor cells, and  $a_6$  represents the rate at which tumor cells inactivate hunting CTLs.  $a_4$  represents the rate at which resting CTLs become hunting cells.  $a_5$  and  $a_{10}$  indicate the rates of apoptosis of hunting and resting cells, respectively. The resting CTLs intrinsic growth rate is  $a_7$ , and its carrying capacity is  $a_8$ . The rate at which a resting CTL makes contact

with a hunting cell is denoted by  $a_9$ .  $a_{11}$  represents the resting CTLs poliferation rate, and  $a_{12}$  represents the steepness coefficient. To reduce the number of parameters in the system, we consider the following non-dimensional variables  $X=a_2x$ ,  $Y=a_2y$ ,  $Z=a_8z$ ,  $\tau=\frac{t}{a_2a_3}$ , and  $\eta_1=\frac{a_1}{a_2a_3}$ ,  $\beta_1=\frac{a_4a_8}{a_2a_3}$ ,  $\gamma_1=\frac{a_5}{a_2a_3}$ ,  $\rho=\frac{a_6}{a_3}$ ,  $\eta_2=\frac{a_7}{a_2a_3}$ ,  $\beta_2=\frac{a_9}{a_3}$ ,  $\gamma_2=\frac{a_{10}}{a_2a_3}$ ,  $\gamma_3=\frac{a_{11}}{a_2a_3}$ ,  $\gamma_3=\frac{a_{12}}{a_2}$ . Then, we obatined the modified form of the system (3.1) as follows:

$$\frac{dx}{dt} = \eta_1 x(1-x) - xy, \quad \frac{dy}{dt} = \beta_1 yz - \gamma_1 y - \rho xy, \quad \frac{dz}{dt} = \eta_2 z(1-z) - \beta_2 yz - \gamma_2 z + \frac{vxz}{x+\delta}. \tag{3.2}$$

# 3.1. Mathematical model with the Caputo-Fabrizio fractional derivative

A unique formulation of the fractional derivative with a non-singular kernel was developed by Caputo and Fabrizio [6]. Unlike classical derivatives that focus only on the local rate of change, the Caputo-Fabrizio derivative incorporates a non-local memory kernel. This kernel weights the entire past history of the system without introducing singularities. The motivation behind interest in this novel technique is that it allows for describing the processes, where the current state depends on the cumulative effects of past events. The kernel in the Caputo-Fabrizio derivative uses an exponential decay function, which ensures a smooth transition of memory effects. This reflects physical systems where memory influence diminishes over time in a controlled manner, rather than abruptly. The incorporation of the Caputo-Fabrizio derivative to the tumor model can be justified in the present context.

- 1. **Memory effects in immune response:** The interactions between tumor cells, hunting cells, and resting CTLs involve memory-dependent processes. For example:
  - hunting cells and resting CTLs rely on immunological memory to recognize and target tumor cells;
  - tumor cells adapt and evolve based on past interactions with the immune system.

The Caputo-Fabrizio derivative integrates these memory effects through an exponential kernel, enabling the model to account for the influence of past dynamics on current behavior.

- 2. Non-singular kernel for biological realism: The Caputo-Fabrizio derivative's non-singular exponential kernel ensures that memory effects decay smoothly over time. This is biologically realistic because:
  - immune memory does not persist indefinitely but diminishes gradually as the immune system resets or tumor cells evade recognition;
  - cellular signaling has a time-limited influence on immune cell behavior.

#### 3. Capturing non-local interactions

- tumor cells interact with hunting cells and resting CTLs through chemical signals, cell-to-cell contact, and extracellular matrix modifications, all of which are inherently non-local;
- the Caputo-Fabrizio derivative allows for modeling these interactions over time and space, accounting for how past and distant events affect current states.

#### 4. Dynamic interplay between players

- Tumor Cells: Compete for resources, evade immune detection, and proliferate or die based on their interactions with CTLs and hunting cells.
- Hunting Cells: Detect and attack tumor cells, influenced by their past exposure and the availability of signaling molecules.
- Resting CTLs: Destroy tumor cells via targeted attacks and depend on activation signals and memory of previous encounters.
- The Caputo-Fabrizio derivative captures the dynamic feedback loops and time-dependent interactions between these entities.

The new form with the Caputo-Fabrizio fractional derivative can be obtained by transforming the integerorder model provided in (3.2) as follows:

$$C^{F}D^{\alpha}x(t) = \eta_{1}x(1-x) - xy,$$

$$C^{F}D^{\alpha}y(t) = \beta_{1}yz - \gamma_{1}y - \rho xy,$$

$$C^{F}D^{\alpha}z(t) = \eta_{2}z(1-z) - \beta_{2}yz - \gamma_{2}z + \frac{\nu xz}{x+\delta},$$
(3.3)

where  $\alpha \in (0,1]$  represents the fractional order and the positive initial conditions are  $x(t_0) = x_0$ ,  $y(t_0) = y_0$ ,  $z(t_0) = z_0$ , where  $\eta_1$  represents the growth rate of tumor cells, representing the intrinsic ability of tumor cells to proliferate, and  $\eta_2$  represents the growth rate of resting CTLs, capturing their replenishment via intrinsic immune processes. The hunting cell inactivation rate by the tumor cell is  $\rho$ .  $\beta_1$  denotes the activation rate of hunting CTLs from resting CTLs, describing how efficiently resting CTLs are converted to active hunting CTLs. The death rate of hunting CTLs, indicating the average lifespan of active immune cells, is denoted by  $\gamma_1$ . The death rate of resting CTLs is denoted by  $\gamma_2$ .  $\beta_2$  represents the deactivation rate of resting CTLs from hunting CTLs, reflecting their direct effectiveness in suppressing tumor growth. The resting CTLs propagation rate is denoted by  $\nu$  in the form of the conversion rate of tumor cells into resting CTLs.  $\delta$  is the steepness coefficient.

#### 4. Existence and uniqueness of the solution

In this section, we present the existence and uniqueness of the solution of the system (3.3).

**Theorem 4.1.** *In the region*  $\Phi \times [0,T]$ *, where*  $\Phi = \{(x,y,z) \in \mathbb{R}^3 : ||x|| < \xi_1, ||y|| < \xi_2, ||z|| < \xi_3\}$ *, and*  $T < +\infty$ *, the system* (3.3) *has a solution and it is unique.* 

*Proof.* Let us consider  $L(t) = (x(t), y(t), z(t)), \bar{L}(t) = (\bar{x}(t), \bar{y}(t), \bar{z}(t)),$  and a function

$$G(t, L) = (G_1(t, L), G_2(t, L), G_3(t, L)),$$

where

$$G_1(t,L) = \eta_1 x(1-x) - xy, \quad G_2(t,L) = \beta_1 yz - \gamma_1 y - \rho xy, \quad G_3(t,L) = \eta_2 z(1-z) - \beta_2 yz - \gamma_2 z + \frac{\nu xz}{x+\delta}.$$

Here, G(t,L) is defined on  $\Phi \times [0,T]$  and consider  $q=\sup_{L\in\Phi}\|G(t,L)\|$ . We take the norm as  $\|L(t)\|=\sup_{t\in[0,T]}|L(t)|$ . We will examine that some  $\Omega>0$  exist, such that  $\|G(L)-G(\bar{L})\|\leqslant\Omega\|L-\bar{L}\|$ . Estimate

$$\begin{split} \|G(L) - G(\bar{L})\| &= \|\eta_1 x (1-x) - xy - \eta_1 \bar{x} (1-\bar{x}) \\ &+ \bar{x} \bar{y} + \beta_1 yz - \gamma_1 y - \rho xy - \beta_1 \bar{y} \bar{z} + \gamma_1 \bar{y} + \rho \bar{x} \bar{y} \\ &+ \eta_2 z (1-z) - \beta_2 yz - \gamma_2 z + \frac{\nu xz}{x+\delta} - \eta_2 \bar{z} (1-\bar{z}) + \beta_2 \bar{y} \bar{z} + \gamma_2 \bar{z} - \frac{\nu \bar{x} \bar{z}}{\bar{x}+\delta} \| \\ &= \|\eta_1 ((x-\bar{x}) - (x^2 - \bar{x}^2)) - (xy - \bar{x} \bar{y}) + \beta_1 (yz - \bar{y} \bar{z}) - \gamma_1 (y - \bar{y}) - \rho (xy - \bar{x} \bar{y}) \\ &+ \eta_2 ((z-\bar{z}) - (z^2 - \bar{z}^2)) - \beta_2 (yz - \bar{y} \bar{z}) - \gamma_2 (z - \bar{z}) + \left( \frac{\nu xz}{x+\delta} - \frac{\nu \bar{x} \bar{z}}{\bar{x}+\delta} \right) \| \\ &\leqslant \|\eta_1 ((x-\bar{x}) - (x^2 - \bar{x}^2)) - x (y - \bar{y}) - \bar{y} (x - \bar{x}) + \beta_1 (y (z - \bar{z}) + \bar{z} (y - \bar{y})) - \gamma_1 (y - \bar{y}) \\ &- \rho (x (y - \bar{y}) + \bar{y} (x - \bar{x})) + \eta_2 ((z - \bar{z}) - (z^2 - \bar{z}^2)) - \beta_2 (y (z - \bar{z}) + \bar{z} (y - \bar{y})) \\ &- \gamma_2 (z - \bar{z}) + \nu \left( \frac{x (z - \bar{z})}{\delta (1 + \frac{x}{\delta})} + \frac{\bar{z} (x - \bar{x})}{\delta (1 + \frac{x}{\delta}) (1 + \frac{\bar{x}}{\delta})} \right) \| \\ &\leqslant \left( \eta_1 (1 + 2\xi_1) + \xi_2 (1 + \rho) + \frac{\nu \xi_3}{\delta} \right) \|x - \bar{x}\| + ((1 + \rho)\xi_1 + \xi_3 (\beta_1 + \beta_2) + \gamma_1) \|y - \bar{y}\| \end{split}$$

$$+\left(\frac{\nu\xi_1}{\delta}+\xi_2(\beta_1+\beta_2)+\eta_2(1+2\xi_3)+\gamma_2\right)||z-\bar{z}||.$$

This implies

$$||G(L) - G(\bar{L})|| \le \Omega_1 ||x - \bar{x}|| + \Omega_2 ||y - \bar{y}|| + \Omega_3 |z - \bar{z}||,$$

where

$$\begin{split} &\Omega_1 = \eta_1(1+2\xi_1) + \xi_2(1+\rho) + \frac{\nu\xi_3}{\delta}, \\ &\Omega_2 = (1+\rho)\xi_1 + \xi_3(\beta_1+\beta_2) + \gamma_1, \\ &\Omega_3 = \frac{\nu\xi_1}{\delta} + \xi_2(\beta_1+\beta_2) + \eta_2(1+2\xi_3) + \gamma_2. \end{split}$$

Consider  $\Omega = \max\{\Omega_1, \Omega_2, \Omega_3\}$ . This yields that  $\|G(L) - G(\bar{L})\| \leqslant \Omega \|L - \bar{L}\|$ . By utilising the function G and the  $\alpha^{\text{th}}$ -order fractional integral, a Picard's operator  $\Lambda$  can be made. Consequently, the following equation is obtained as

$$\Lambda L = {}^{CF}I^{\alpha}G(t,L) + L(0). \tag{4.1}$$

The next task is to demonstrate that this operator maps a complete non-empty metric space into itself and that it is a contraction mapping. Consider  $||L - L(0)|| \le \sigma$ . Taking norm on (4.1), we get

$$\|\Lambda L - L(0)\| \le \|G(t, L)\|^{CF} I^{\alpha}(1) \le q \frac{2(1 - \alpha(1 - T))}{A(\alpha)(2 - \alpha)} < \sigma.$$
 (4.2)

The inequality in (4.2) is satisfied, if  $\frac{(1-\alpha(1-T))}{A(\alpha)(2-\alpha)} < \frac{\sigma}{2q}$ . In this case, we obtain a condition under which the operator  $\Lambda$  is a contraction. We give this constraint by following some steps as below:

$$\begin{split} \|\Lambda L - \Lambda \bar{L}\| &= \|^{CF} I^{\alpha}(G(t,L) - G(t,\bar{L}))\| \\ &\leqslant {}^{CF} I^{\alpha} \|G(t,L) - G(t,\bar{L})\| \leqslant \|G(t,L) - G(t,\bar{L})\|^{CF} I^{\alpha}(1) \leqslant \frac{2(1-\alpha(1-T))}{A(\alpha)(2-\alpha)} \Omega \|L - \bar{L}\|. \end{split}$$

The equation above indicates that the Picard's operator  $\Lambda$  becomes a contraction when the relation

$$\frac{(1-\alpha(1-\mathsf{T}))}{\mathsf{A}(\alpha)(2-\alpha)}\leqslant \frac{1}{2\Omega},$$

holds. This establishes the contractive nature of Picard's operator  $\Lambda$ . The Banach fixed point theorem states that the operator  $\Lambda$  has a unique fixed point, which means that the fractional transformed system (3.3) has a unique solution. In this case, we have

$$\frac{(1-\alpha(1-T))}{A(\alpha)(2-\alpha)} < \min\left\{\frac{\sigma}{2q}, \frac{1}{2\Omega}\right\},$$

and the proof is complete.

#### 5. Circuit implementation of the Simulink model in MATLAB

To establish a concrete bridge between theoretical modeling and experimental interpretation, the proposed electronic circuit implementation acts as an analog simulation platform for the nonlinear dynamics of tumor-immune interactions represented by the model (3.3). The suggested 3D chaotic model (3.3) of integer order  $\alpha = 1$  is taken into consideration in order to design a circuit.

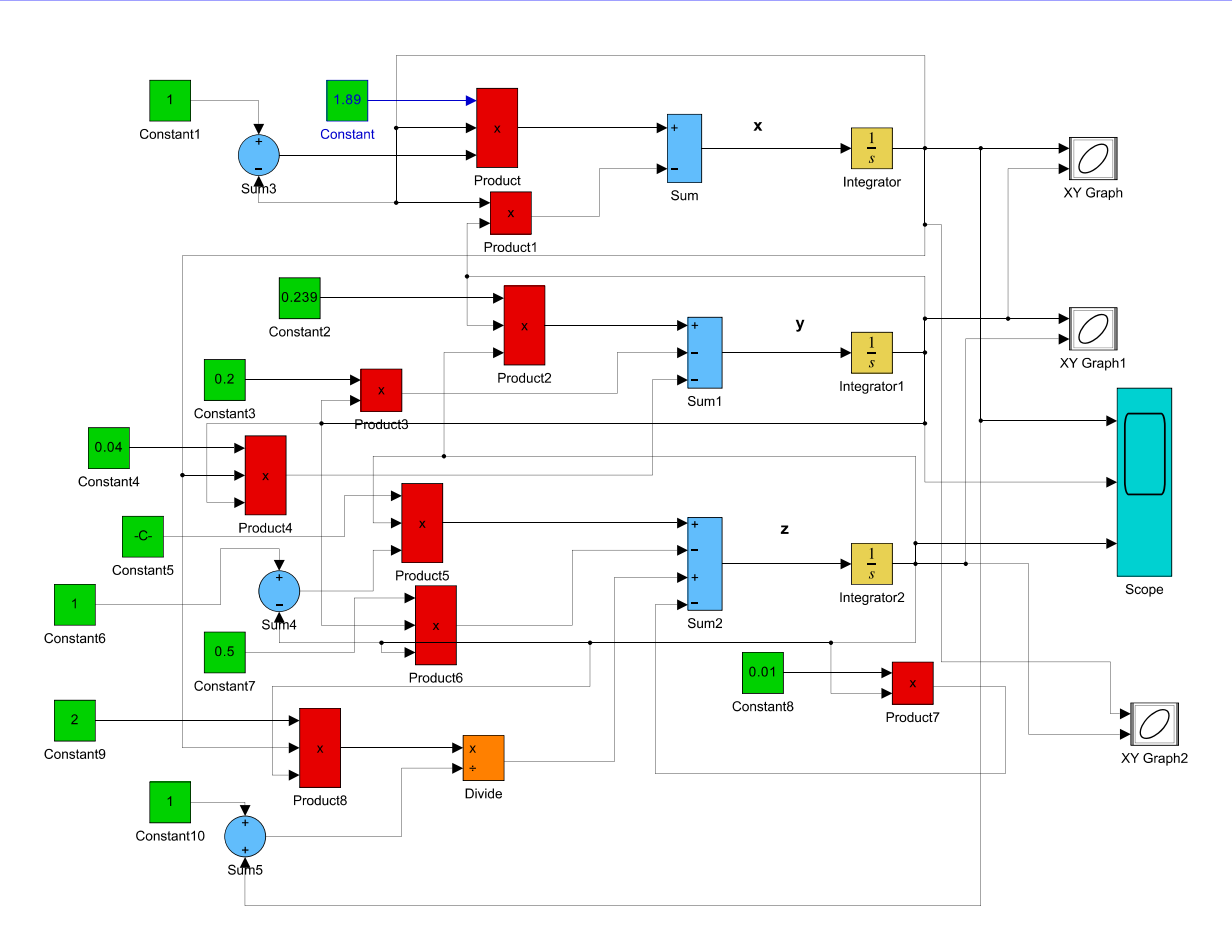


Figure 1: Lab view of circuit in Simulink.

Three integrators are incorporated into the model to generate a Matlab-Simulink model for the system of nonlinear equations (3.3):

$$x = \int (1.89x(1-x) - xy) dt,$$

$$y = \int (0.239yz - 0.2y - 0.04xy) dt,$$

$$z = \int (0.0691z(1-z) - 0.5yz - 0.01z + \frac{2xz}{x+1}) dt.$$
(5.1)

In this framework, the circuit voltages represent scaled versions of biologically significant variables: tumor cell density (x), activated cytotoxic T lymphocytes (CTLs) (y), and resting CTLs (z). These voltages evolve according to the nonlinear interactions encoded in the system of differential equations. For instance, a rise in the voltage representing x reflects tumor proliferation, while changes in y and z correspond to activation or suppression of immune responses. Such analog modeling enables rapid and continuous simulation of tumor-immune dynamics under varying conditions, offering a potential tool for detailed experimentation, biomedical education, and prototype testing of control strategies. This physical interpretability enhances the practical relevance of the mathematical model and supports its application in real-world scenarios. The Matlab-Simulink model (5.1) is schematically depicted in Figure 1. In addition to interconnected amplification blocks, it has signal recording devices such as multiplication, integration, summation, subtraction, and division. So, we have

$$\dot{\mathbf{x}} = (1.89\mathbf{x}(1-\mathbf{x}) - \mathbf{x}\mathbf{y}), \quad \dot{\mathbf{y}} = (0.239\mathbf{y}z - 0.2\mathbf{y} - 0.04\mathbf{x}\mathbf{y}), \quad \dot{\mathbf{z}} = (0.0691z(1-z) - 0.5\mathbf{y}z - 0.01z + \frac{2\mathbf{x}z}{\mathbf{x}+1}).$$

Directly implementing model (3.3) with an electronic circuit presents an additional challenge. Equation (3.3) provides a wide dynamic range of fluctuating variables with values that exceed suitable power supply restrictions. Operational amplifiers' operating voltage range in real electrical circuits is typically between -15V and +15V. The parameter values are considered as  $\eta_1 = 1.89$ ,  $\eta_2 = 0.0691$ ,  $\beta_1 = 0.239$ ,  $\beta_2 = 0.5 \gamma_1 = 0.2$ ,  $\gamma_2 = 0.01$ ,  $\nu = 2$ ,  $\rho = 0.04$ ,  $\delta = 1$  [17] and the initial conditions are  $\kappa(0) = 0.4$ ,  $\kappa(0) = 1$ ,  $\kappa(0) = 0.1$ . It is possible to see the outcomes of modeling the chaotic system (3.3) in MATLAB-Simulink and LabVIEW by comparing the time graph in Figure 3 and Figures 5 (a). Figure 2 represents the 2D view of the components' relations generated in Matlab-Simulink and LabVIEW, which in turn resembles the 2D view displayed in Figure 4 generated from model (3.3) using the Adams-Bashforth method aided by Mathematica.

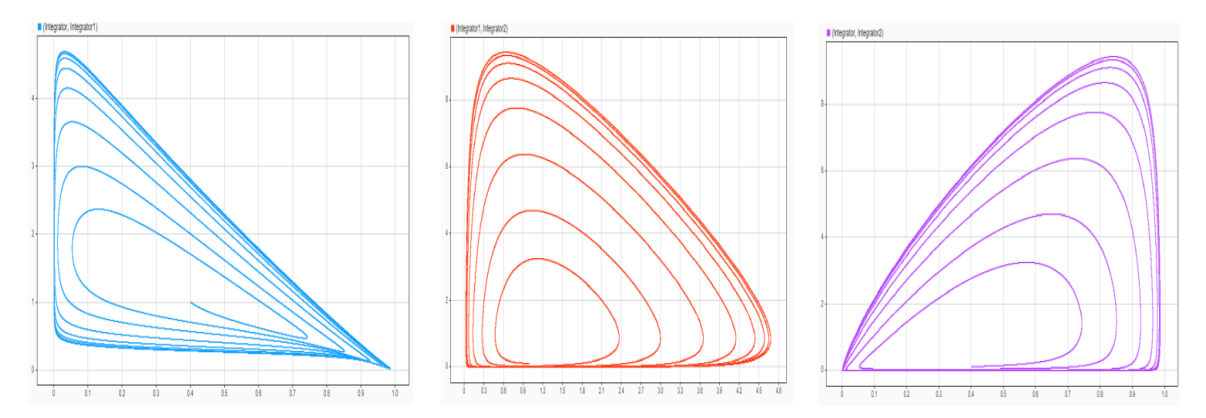


Figure 2: x - y, y - z, x - z plane of cancer model circuit analysis in Simulink.

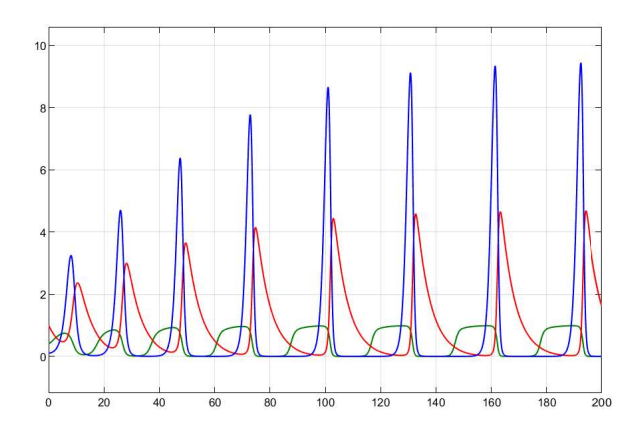


Figure 3: Circuit analysis time graph for model 7 in Simulink.

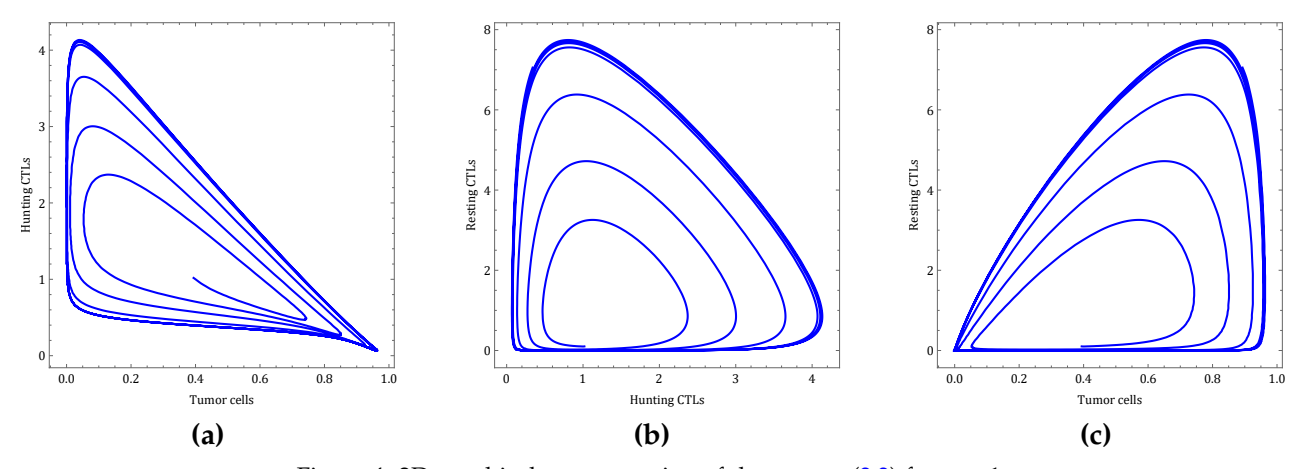


Figure 4: 2D graphical representation of the system (3.3) for  $\alpha=1.$ 

#### 6. Dynamics of the system (3.3)

The system (3.3) has five biologically viable equilibrium points. In this section, we shall analyze their existence and stability conditions relying on some threshold parameters. The Jacobian matrix at any arbitrary point, E(x, y, z) is computed in order to accomplish this:

$$J = \begin{pmatrix} b_{11} & b_{12} & b_{13} \\ b_{21} & b_{22} & b_{23} \\ b_{31} & b_{32} & b_{33} \end{pmatrix},$$

where,

$$\begin{array}{ll} b_{11} = -y + \eta_1(1-2x), & b_{12} = -x, & b_{13} = 0, \\ b_{21} = -\rho y, & b_{22} = -\rho x + \beta_1 z - \gamma_1, & b_{23} = \beta_1 y, \\ b_{31} = \frac{\nu x}{x+\delta} - \frac{\nu xz}{(x+\delta)^2}, & b_{32} = -\beta_2 z, & b_{33} = \frac{\nu x}{x+\delta} - \beta_2 y - \gamma_2 + \eta_2 (1-2z). \end{array}$$

- 1. First boundary equilibrium point is  $E_1(1,0,0)$  and it exists for any set of parameter values.
- 2. Another boundary equilibrium point is  $E_2(0,0,z_2)$ , where  $z_2=1-\frac{\gamma_2}{\eta_2}=\frac{\gamma_2}{\eta_2}(R_0-1)$ , and  $R_0=\frac{\eta_2}{\gamma_2}$ . If  $\eta_2>\gamma_2$ , then  $R_0>1$  and it biologically holds, because proliferation of the resting cell is greater than the natural decay of the resting cell. Hence,  $E_2$  is non-negative.
- 3. The tumor free equilibrium point is  $E_3(0,y_3,z_3)$ , where  $y_3=\frac{\eta_2}{\beta_2}(1-R_1)$ ,  $z_3=\frac{\gamma_1}{\beta_1}$ , and  $R_1=\frac{\gamma_2}{\eta_2}+\frac{\gamma_1}{\beta_1}$ . If  $R_1<1$ , then  $E_3$  exists.
- 4. The equilibrium point  $E_4(x_4,0,z_4)$  represents a situation when there are no hunting cell. Here  $x_4=1$  and  $z_4=\frac{\gamma_2}{\eta_2}\left(R_2-1\right)$ , where  $R_2=\frac{\eta_2}{\gamma_2}+\frac{\nu}{\gamma_2(1+\delta)}$ . If  $R_2>1$ , then  $E_4$  exists.
- 5. The interior equilibrium point is  $E_5 = (x_5, y_5, z_5)$ . Furthermore, we obtain a polynomial of degree three by removing y and z from the system of equations (3.3), we get

$$Q_1 x^2 + Q_2 x + Q_3 = 0, (6.1)$$

where

$$\begin{split} Q_1 &= \beta_1 \beta_2 \eta_1 - \rho \eta_2, \\ Q_2 &= \beta_1 (\nu + \eta_2 - \gamma_2) + \beta_1 \beta_2 \eta_1 (\delta_1) - \eta_2 (\gamma_1 + \rho \delta), \\ Q_3 &= -(\delta \beta_1 (\gamma_2 + \beta_2 \eta_1) + \delta \gamma_1 \eta_2). \end{split}$$

Clearly  $Q_3$  is negative. Therefore, the system (6.1) has at least one positive real root. Hence interior equilibrium point  $E_5$  exists.

## 6.1. Stability

**Theorem 6.1.** Boundary equilibrium point  $E_1$  is a saddle point.

*Proof.* The eigen-values of the Jacobian matrix J of the system (3.3) at  $E_1$  are as follows:

$$\lambda_{11}=-(\rho+\gamma_1),\quad \lambda_{12}=-\eta_1,\quad \lambda_{13}=\frac{\nu}{1+\delta}+\gamma_2(R_0-1).$$

 $\lambda_{11}$  and  $\lambda_{12}$  are real and negative. Since the growth rate of the resting cell is greater than the natural decay of the resting cell,  $R_0 > 1$  is a biologically meaningful statement. Hence,  $\lambda_{11} > 0$  and this leads  $E_1$  to be a saddle point.

**Theorem 6.2.** *The boundary equilibrium point*  $E_2$  *is always saddle.* 

*Proof.* The eigen-values of the Jacobian matrix J of the system (3.3) at  $E_2$  are as follows:

$$\lambda_{21} = \eta_1, \quad \lambda_{22} = \gamma_2(1 - R_0), \quad \lambda_{23} = -\frac{\beta_1 \gamma_2}{\eta_2}(1 - R_0) + \gamma_1.$$

Existence of  $E_2$  demands that  $R_0 > 1$ . Clearly  $\lambda_{21}$  and  $\lambda_{23}$  are real and positive, and  $\lambda_{22}$  is real and negative for any set of parameter values. Hence,  $E_2$  is always a saddle point.

**Theorem 6.3.** Let  $\tilde{R}_1 = \frac{\beta_1\beta_2\eta_1 + \gamma_1\eta_2}{\beta_1\gamma_2(R_0-1)}$ . The tumor free equilibrium point  $E_3$  is stable if  $\tilde{R_1} > 1$  and  $R_1 + \frac{\gamma_1^2}{4\beta_1^2} < 1$ .

*Proof.* The following values are the eigen-values of the Jacobian matrix J at  $E_3$  for the system (3.3):

$$\begin{split} \lambda_{31} &= \frac{\beta_1 \gamma_2 + \beta_1 \beta_2 \eta_1 - \beta_1 \eta_2 + \gamma_1 \eta_2}{\beta_1 \beta_2} = \frac{\gamma_2}{\beta_2} (R_0 - 1) (1 - \tilde{R_1}), \\ \lambda_{32} &= -\frac{\gamma_1 \eta_2}{2\beta_1} - \sqrt{\eta_2 \gamma_1} \sqrt{(R_1 - 1) + \frac{\gamma_1^2}{4\beta_1^2}}, \\ \lambda_{33} &= -\frac{\gamma_1 \eta_2}{2\beta_1} + \sqrt{\eta_2 \gamma_1} \sqrt{(R_1 - 1) + \frac{\gamma_1^2}{4\beta_1^2}}. \end{split}$$

 $\lambda_{31}$  is negative, if  $\tilde{R}_1 > 1$ . When  $R_1 + \frac{\gamma_1^2}{4\beta_1^2} < 1$ , it indicates that the eigen-values  $\lambda_{32}$  and  $\lambda_{33}$  are complex conjugate with negative real parts.

**Theorem 6.4.** Let  $\tilde{R}_2 = \frac{\beta_1(\nu + \gamma_2(R_0 - 1)(1 + \delta))}{\eta_2(1 + \delta)(\rho + \gamma_2)}$ . The equilibrium point  $E_4$  is stable if  $\tilde{R}_2 > 1$ .

*Proof.* The eigen-values of the Jacobian matrix J of the system (3.3) at  $E_4$  are as follows:

$$\lambda_{41} = -\eta_1, \quad \lambda_{42} = -\left(\frac{\nu + \gamma_2(R_0 - 1)(1 + \delta)}{1 + \delta} + \right), \quad \lambda_{43} = (\rho + \gamma_2)(1 - \tilde{R}_2).$$

Clearly,  $|arg(\lambda_{41})| = \pi > \frac{\alpha\pi}{2}$  and  $|arg(\lambda_{42})| = \pi > \frac{\alpha\pi}{2}$ . Hence  $E_4$  is stable if  $|arg(\lambda_{43})| > \frac{\alpha\pi}{2}$ . The fundamental conditions for this is  $\tilde{R_2} > 1$ .

**Theorem 6.5.** If  $L_1L_2 - L_3 > 0$ , then the co-existence equilibrium point  $E_5$  is locally stable.

*Proof.* The variational matrix corresponding to E<sub>5</sub> is

$$J(x_5, y_5, z_5) = (n_{ij})_{3\times 3}, \quad i, j = 1, 2, 3, \tag{6.2}$$

where,

$$\begin{split} &n_{11}=-y_5+\eta_1(1-2x_5), &n_{12}=-x_5, &n_{13}=0, \\ &n_{21}=-\rho y_5, &n_{22}=-\rho x_5+\beta_1 z_5-\gamma_1, &n_{23}=\beta_1 y_5, \\ &n_{31}=\frac{\nu x_5}{x_5+\delta}-\frac{\nu x_5 z_5}{(x_5+\delta)^2}, &n_{32}=-\beta_2 z_5, &n_{33}=-\left(\beta_2 y_5+\gamma_2+\eta_2(2z_5-1)-\frac{\nu x_5}{x_5+\delta}\right). \end{split}$$

Thereafter the characteristic equation of equation (6.2) is

$$\lambda^3 + L_1 \lambda^2 + L_2 \lambda + L_3 = 0, (6.3)$$

where,

$$\begin{split} L_1 &= -(n_{11} + n_{22} + n_{33}), \\ L_2 &= n_{33}(n_{11} + n_{22}) - (n_{12}n_{21} - n_{11}n_{22}) - n_{23}n_{32}, \\ L_3 &= n_{33}(n_{12}n_{21} - n_{11}n_{22}) + n_{23}(n_{12}n_{31} - n_{11}n_{32}), \\ L_1L_2 - L_3 &= n_{22}(n_{21}n_{22} + n_{23}n_{31}) + (n_{22} + n_{33})(n_{23}n_{32} - n_{22}n_{33} - n_{11}^2) + n_{11}(n_{12}n_{21} - (n_{22} + n_{33})^2). \end{split}$$

Thus, in the basis of the Routh-Hurwitz criteria, if  $n_{11} < 0$ ,  $(n_{11} + n_{22}) < 0$ ,  $(n_{12}n_{21} - n_{11}n_{22}) < 0$ , when  $L_1L_2 - L_3 > 0$ , the coefficients of equation (6.3) are strictly positive, meaning that the coexisting equilibria  $E_5$  are locally stable.

## 6.2. Threshold dynamics

In this work, we have defined four threshold parameters to analyze the dynamics of the equilibrium points.

- 1.  $R_0 = \frac{\eta_2}{\gamma_2}$ .  $\eta_2$  denotes the growth rate of resting cell and  $\frac{1}{\gamma_2}$  denotes the average life span of resting cell. Their product quantifies the average number of resting cells maintained in the population by the growth process over time. Therefore,  $R_0$  represents the basic reproduction number (BR) of resting cells in the absence of tumor cells and hunting cells. For the existence of  $E_2$ , this BR number must be greater than 1.
- 2. The ratio  $\frac{\gamma_2}{\eta_2}$  reflects the inverse contribution of resting CTLs to tumor suppression. A higher value indicates that resting CTLs are less effective in controlling tumor cells, as their population is unable to sustain itself due to a high death rate or low replenishment rate. Conversely, a lower value suggests a more robust resting CTL population capable of exerting consistent pressure on tumor cells. The ratio  $\frac{\gamma_1}{\beta_1}$  captures the inverse effectiveness of hunting CTLs in tumor suppression. A higher value indicates that hunting CTLs are less efficient at reducing tumor cells, either due to a high death rate or a low tumor-killing rate. A lower value suggests that hunting CTLs are effectively controlling tumor growth. A lower  $R_1$  indicates a stronger immune response, where resting and hunting CTLs collectively exert significant pressure on tumor cells, leading to tumor suppression. A higher  $R_1$  suggests reduced immune efficiency, where either resting or hunting CTLs (or both) are unable to adequately control tumor growth due to high death rates or low functional efficiency.
- 3. Tumor-free equilibrium point.  $R_1$  quantifies the balance between the death and activation rates of immune cells, as well as their capacity to sustain a robust immune response. If  $R_1 < 1$ , the immune system is well-balanced, with sufficient resting and hunting CTLs to counteract tumor dynamics. Hence, it is justified that the existence of a tumor-free equilibrium point requires  $R_1 < 1$ .
  - The product  $\beta_1\beta_2\eta_1$  quantifies the tumor-induced immune response and reflects how tumor growth influences the activation and effectiveness of hunting CTLs.
  - The product  $\gamma_1\eta_2$  reflects the baseline immune response from the growth of resting CTLs and the natural turnover of hunting CTLs.
  - The numerator  $\beta_1\beta_2\eta_1 + \gamma_1\eta_2$  quantifies the immune system's ability to respond to tumor growth, considering both activation  $\beta_1$ , deactivation  $\beta_2$ , and decay  $\gamma_1$ .
  - The product  $\beta_1\gamma_2$  represents the interaction between activation and decay processes.  $\beta_1\gamma_2(R_0-1)$  modulates this response by reflecting the sustainability of the resting CTL population, which is the precursor for immune activation.

The term  $\tilde{R}_1$  integrates tumor growth, immune activation, and CTL decay dynamics to measure the tumor-immune system's overall state. It highlights the competing effects of tumor proliferation, immune activation, deactivation, and decay. A high  $\tilde{R}_1$  indicates an effective immune response, while a low  $\tilde{R}_1$  points to vulnerabilities in the immune system. Hence,  $\tilde{R}_1 > 1$  indicates that the immune response is effective enough to counterattack the tumor cell. The term  $\frac{\gamma_1^2}{4\beta_1^2}$  is derived from

the dynamics of hunting CTLs. A smaller  $\frac{\gamma_1^2}{4\beta_1^2}$  implies that hunting CTLs are more effective because their death rate is relatively low compared to their activation rate. It adds an additional layer of stability. The inequality  $R_1 + \frac{\gamma_1^2}{4\beta_1^2} < 1$  indicates that the immune system is operating in a regime where the balance between immune cell dynamics and tumor cell suppression is favorable.

4.  $R_2 = \frac{\eta_2}{\gamma_2} + \frac{\nu}{\gamma_2(1+\delta)}$ .  $\nu$  represents the conversion rate of tumor cells to resting cells.  $\frac{1}{\gamma_2(1+\delta)}$  represents the adjusted average life span of resting cells, where the death rate is modulated by a factor related to the steepness coefficient  $\delta$ . When the expression is considered cumulatively as  $\frac{\nu}{\gamma_2(1+\delta)}$ , it reflects the aggregate behavior over time of how tumor cells transition into resting cells, considering the competing dynamics of resting cell death and the modulation by the steepness coefficient. Again,

 $\frac{\Pi^2}{\gamma_2}$  represents the average number of resting cells maintained in the population by the growth process over time. Hence, in this context,  $R_2$  reflects the effective basic reproduction number of resting CTLs in the presence of tumor cells, representing their overall ability to persist and respond under the influence of both intrinsic and extrinsic factors. When  $R_2 > 1$ , the immune system is better equipped to maintain a stable resting CTL population, enhancing its capacity to combat tumor growth. Conversely, lower values of  $R_2$  may indicate insufficient resting CTLs, potentially leading to immune system destabilization and tumor progression. In the numerator of  $\tilde{R}_2$ , the combined term reflects the contribution of resting CTLs' dynamics, particularly their loss and modulation, to the immune system's overall capacity to manage tumor growth. On the other hand, the denominator of  $\tilde{R}_2$  represents the constraints on the immune system's capacity, including how efficiently it replenishes resting CTLs and their turnover dynamics. Cumulatively,  $\tilde{R}_2$  measures the balance between the immune system's ability to activate hunting CTLs, manage tumor conversion, and maintain resting CTL dynamics relative to the limitations imposed by resting CTL growth and turnover. A higher  $\tilde{R}_2$  indicates a robust immune response, while a lower  $\tilde{R}_2$  signals a weakened capacity to handle tumor growth. For the stability of the system at  $E_4$ , the condition  $\tilde{R}_2 > 1$  is validated.

#### 7. Results and discussion

In this section, extensive numerical simulations are carried out to investigate the dynamic behavior of the proposed cancer model using the generalized predictor-corrector method [4, 8]. The model's dynamics are explored by employing parameter values:  $\eta_1=1.89$ ,  $\beta_1=0.239$ ,  $\gamma_1=0.2$ ,  $\rho=0.04$ ,  $\eta_2=0.0691$ ,  $\beta_2=0.5$ ,  $\gamma_2=0.01$ ,  $\nu=2$ ,  $\delta=1$  [17]. These simulations highlight the effects of varying the fractional-order operator  $\alpha$  on the system's sub-populations, including tumor cells, resting CTLs, and hunting CTLs. Graphs depicting the fluctuation of these sub-populations over time for varying fractional-order values  $\alpha$  are presented in Figures 5-15. These figures demonstrate how changes in  $\alpha$  and other parameter values influence the stability and oscillatory behavior of the tumor-immune system.

#### 7.1. Influence of fractional order $\alpha$

The system exhibits instability when the density of resting cells is high. However, as the density of resting cells decreases, the system tends to stabilize under the influence of the fractional-order  $\alpha$ . This phenomenon, illustrated in Figure 5, reveals that lower values of  $\alpha$  contribute to a gradual stabilization of the system. Additionally, Figure 5 shows that the density of hunting cells increases as  $\alpha$  decreases. This increase in hunting cell density facilitates the system's convergence toward stability. An essential advantage of fractional differential equations over their integer-order counterparts is their broader stability range. This enhanced stability range is evident in the results, as shown in Figure 6. For decreasing values of  $\alpha$ , the system exhibits increased stability, indicating a pronounced memory effect. This memory effect reflects the system's reliance on its historical states, a characteristic feature of fractional-order systems.

# 7.2. Effect of tumor growth rate $(\eta_1)$

Figures 7-9 investigate the impact of tumor cell growth rate  $(\eta_1)$  on the system dynamics for fixed values of  $\alpha$ . For integer-order systems  $(\alpha=1)$ , the model remains unstable across various tumor growth rates. However, as  $\alpha$  moves away from unity, the system transitions through stable limit cycles before eventually converging to stability at  $\alpha=0.7$ . These results underline the critical role of fractional-order  $\alpha$  in moderating the effects of tumor growth rate and guiding the system toward stability. Biologically, this implies that memory and history-dependent processes, captured mathematically by the fractional-order derivative, can enhance the immune system's ability to contain or eliminate tumor cells, even under conditions of high proliferation. The stabilizing influence of lower  $\alpha$  values may reflect biological phenomena such as immune memory, delayed cellular responses, or accumulated immune adaptations, which are absent in integer-order models.

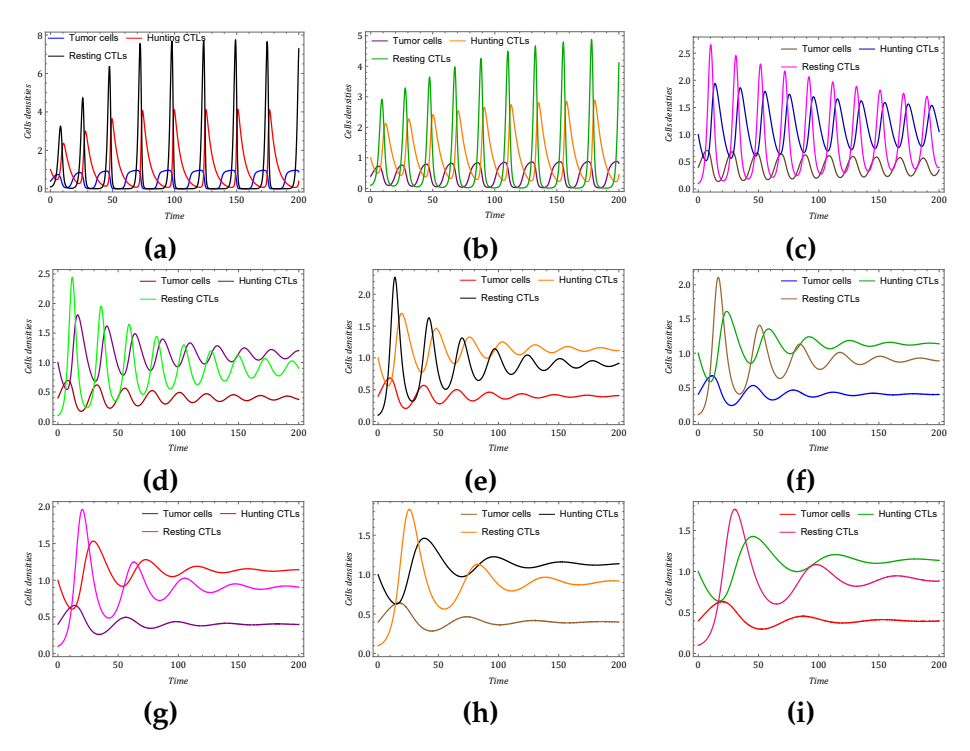


Figure 5: Time progressive trajectories of the system (3.3) for  $\alpha = 1, 0.9, 0.8, 0.7, 0.6, 0.5, 0.4, 0.3,$  and 0.25.

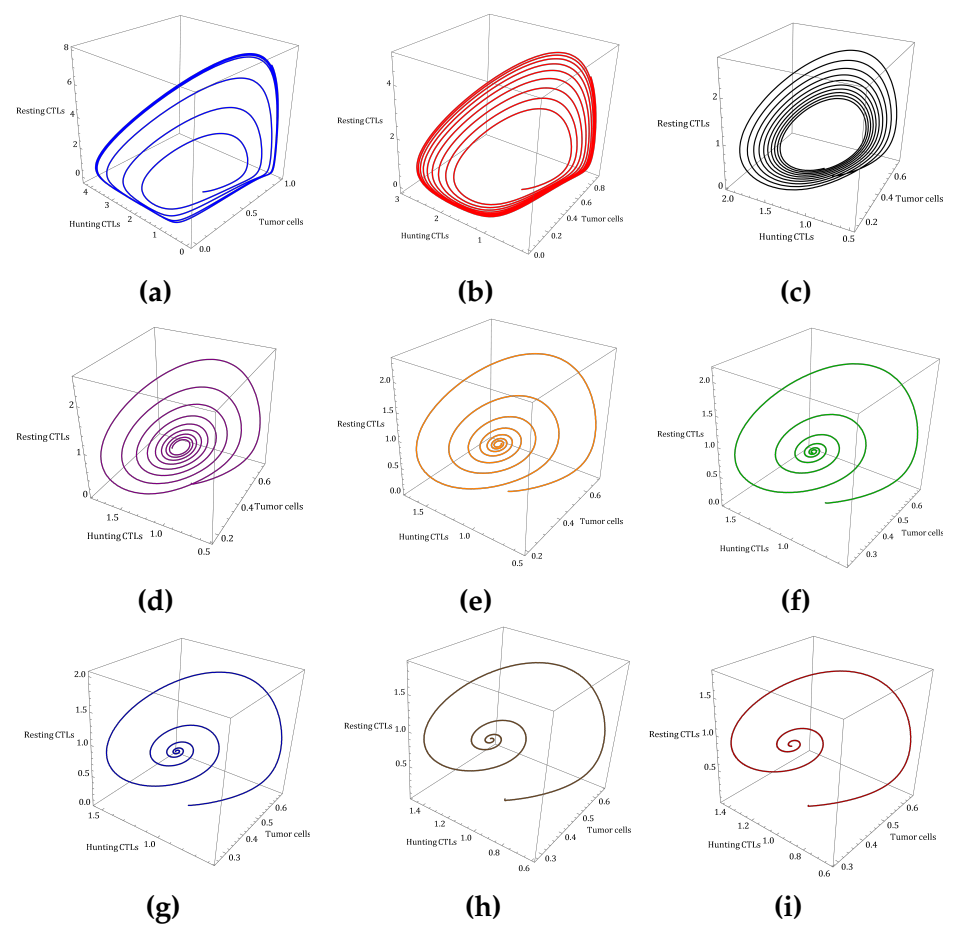


Figure 6: Dyanmics of the system (3.3) for  $\alpha = 1, 0.9, 0.8, 0.7, 0.6, 0.5, 0.4, 0.3,$  and 0.25.

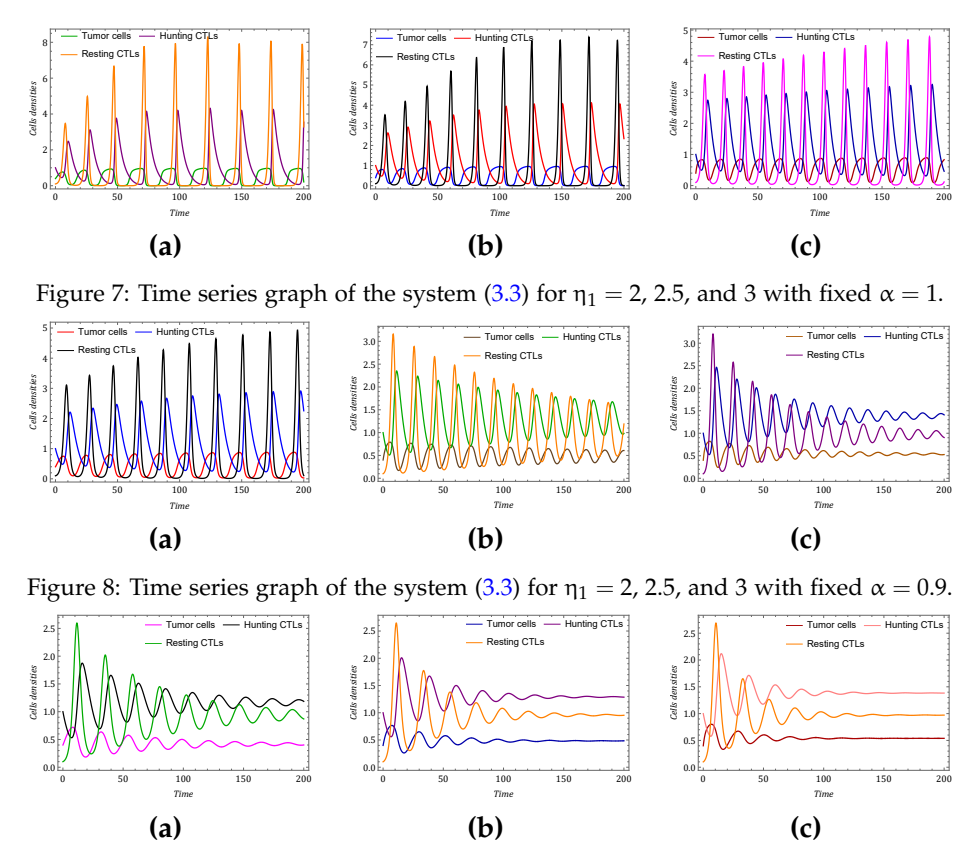


Figure 9: Time series graph of the system (3.3) for  $\eta_1 = 2$ , 2.5, and 3 with fixed  $\alpha = 0.7$ .

#### 7.3. Role of steepness coefficient $(\delta)$

The steepness coefficient  $\delta$  significantly influences the system dynamics, as depicted in Figures 10-12. Increasing values of  $\delta$  lead to higher tumor cell densities while reducing the densities of both resting and hunting cells. Biologically, a higher  $\delta$  reduces the efficiency of this conversion process, meaning that as tumor burden increases, the immune system responds more weakly. This imbalance causes the system to exhibit more oscillatory behavior in the integer-order case ( $\alpha=1$ ). However, as  $\alpha$  decreases, the number of oscillations diminishes, and the system becomes progressively stable. These findings highlight  $\delta$ 's critical role in shaping the dynamics of the tumor-immune system and its interplay with fractional-order effects.

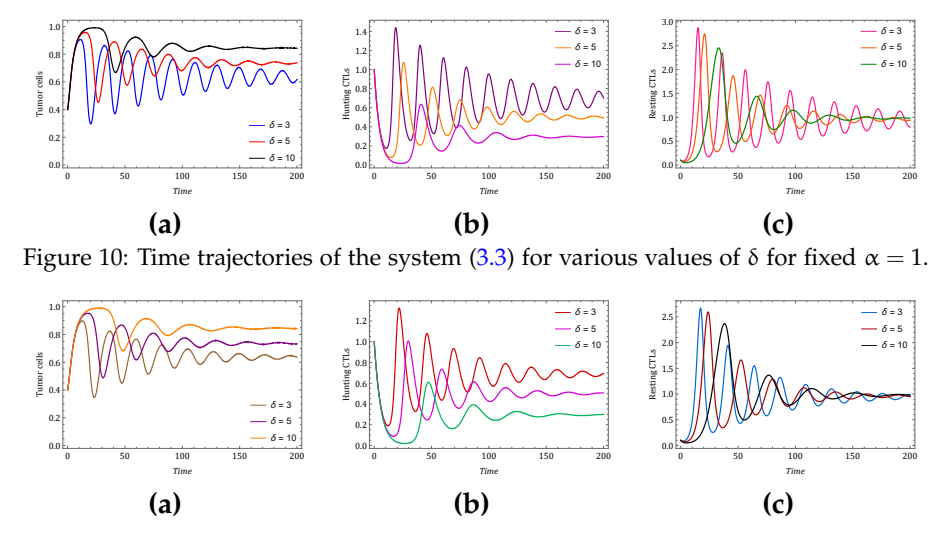


Figure 11: Time trajectories of the system (3.3) for various values of  $\delta$  for fixed  $\alpha = 0.9$ .

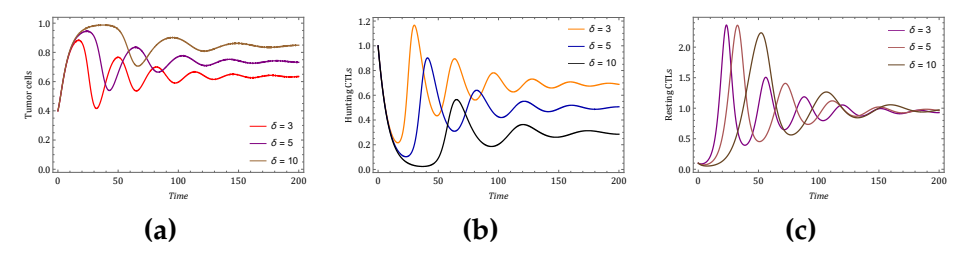


Figure 12: Time trajectories of the system (3.3) for various values of  $\delta$  for fixed  $\alpha = 0.7$ .

#### 7.4. Impact of resting cell growth rate $(\eta_2)$

Figures 13-15 explore the influence of resting cell growth rate  $(\eta_2)$  on the system dynamics. For  $\eta_2=0.0491$  and  $\alpha=1$ , the system exhibits instability with pronounced oscillations. This suggests that when the immune system lacks a sufficient baseline generation of resting CTLs, it fails to maintain control over tumor growth, resulting in fluctuating dynamics and persistent immune-tumor conflict. However, as  $\alpha$  takes on fractional values, the number of oscillations decreases, and the system stabilizes. Moreover, higher growth rates of resting cells  $(\eta_2)$  significantly impact the system's stability. Increasing  $\eta_2$  shifts the system dynamics toward stability, particularly when combined with lower fractional-order values. This aligns with biological observations where immune memory and delayed responses can compensate for limited immediate immune availability, providing more robust long-term regulation.

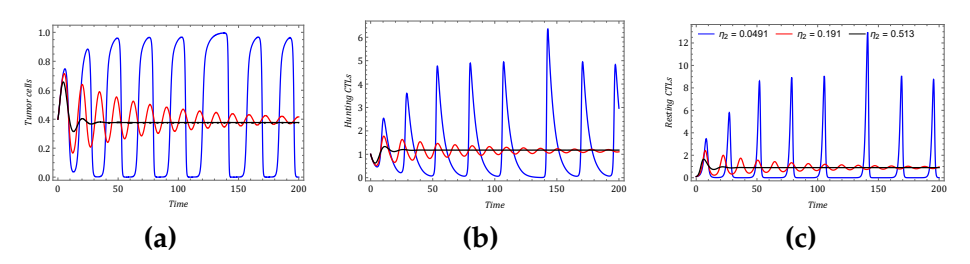


Figure 13: Time versus tumor cells, hunting CTLs and resting CTLs for various values of  $\eta_2$  for fixed  $\alpha=1$ .

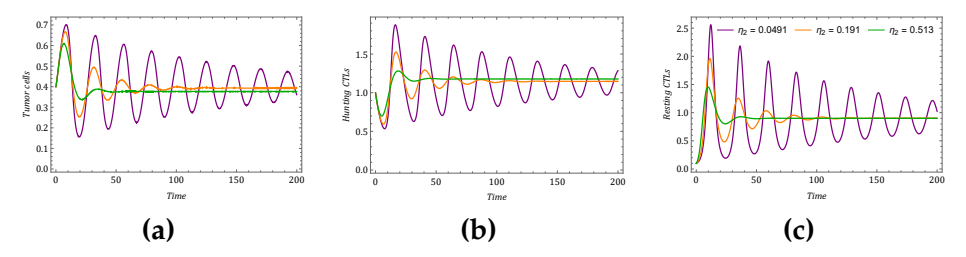


Figure 14: Time versus tumor cells, hunting CTLs and resting CTLs for various values of  $\eta_2$  for fixed  $\alpha = 0.7$ .

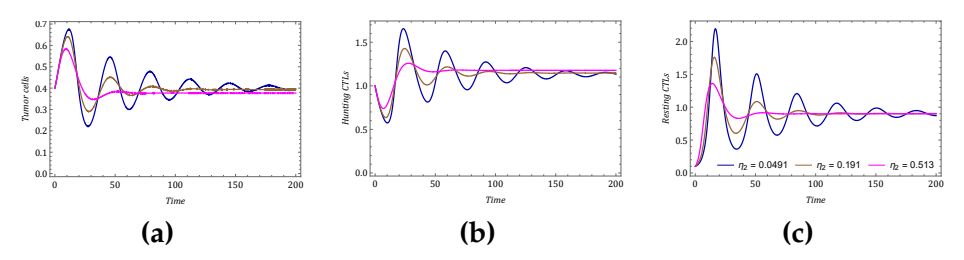


Figure 15: Time versus tumor cells, hunting CTLs and resting CTLs for various values of  $\eta_2$  for fixed  $\alpha = 0.5$ .

## 7.5. Key observations

The simulations clearly demonstrate that fractional-order  $\alpha$  plays a vital role in stabilizing the tumor-immune system. By reducing  $\alpha$  from unity, the system transitions from instability to stability, reflecting

the memory effect inherent in fractional differential equations. Additionally, the parameters  $\eta_1$ ,  $\eta_2$ , and  $\delta$  have critical influences on the tumor-immune dynamics. The findings suggest that tuning these parameters, along with adjusting  $\alpha$ , could provide valuable insights for modeling and potentially controlling tumor progression. The numerical results, validated by theoretical analyses, underscore the significance of fractional-order systems in capturing the complex dynamics of tumor-immune interactions. The broader stability range and memory effects of fractional-order models offer an improved framework for studying biological systems, with implications for cancer research and treatment strategies.

#### 8. Conclusion

This paper employs the Caputo-Fabrizio fractional derivative to analyze the interaction between immune system components, modeling tumor cells as prey and resting and hunting CTLs as predators. The existence of a solution has been proven, the equilibrium points of the system identified, and their local stability assessed using the Banach fixed-point theorem. To further understand the dynamics of the system, mathematical analyses and parameter recalibration studies were conducted. In addition to numerical simulations of the proposed model, which depict the population dynamics of the tumor-immune system under varying fractional orders and estimated parameters using the generalized predictor-corrector approach of Adams type, this work integrates circuit implementations. By translating the theoretical model into a circuit framework in MATLAB, the authenticity and computational precision of the model were validated, offering a novel perspective for understanding the system's behavior. The impact of various factors on the growth and regression of tumor cells was examined through both numerical simulations and circuit-based analyses. This comprehensive approach enhances the reliability of the findings and provides valuable insights into the intricate dynamics of tumor progression and immune response modulation.

# Acknowledgments

This project is sponsored by Prince Sattam Bin Abdulaziz University (PSAU) as part of funding for its SDG Roadmap Research Funding Programme project number PSAU-2023-SDG-19.

#### Authors' contribution

- C. Baishya: conceptualization, formal analysis, methodology, writing-original draft, supervision;
- **R. George:** conceptualization, methodology, writing-review & editing, supervision, project administration;
- R. N. Premakumari: conceptualization, formal analysis, writing-original draft;
- **A. J. Rangappa:** formal analysis, software, writing-original draft;
- S. Etemad: investigation, software, writing-review & editing;
- A. T. Alkhafaji: formal analysis, investigation, writing-review & editing.

#### References

- [1] J. A. Adam, N. Bellomo, A Survey of Models for Tumor-Immune System Dynamics, Springer Science & Business Media, Boston, (1997). 1
- [2] R. F. Alvarez, J. A. M. Barbuto, R. Venegeroles, A nonlinear mathematical model of cell-mediated immune response for tumor phenotypic heterogeneity, J. Theoret. Biol., 471 (2019), 42–50. 1
- [3] L. Anderson, S. Jang, J.-L. Yu, *Qualitative behavior of systems of tumor-CD4*<sup>+</sup>-cytokine interactions with treatments, Math. Methods Appl. Sci., **38** (2015), 4330–4344. 1

- [4] C. Baishya, P. Veeresha, *Dynamics of the Dadras-Momeni system in the frame of the Caputo-Fabrizio fractional derivative*, In: Special functions in fractional calculus and engineering, CRC Press, Boca Raton, FL, (2023), 241-269. 7
- [5] S. Banerjee, R. R. Sarkar, *Delay-induced model for tumor-immune interaction and control of malignant tumor growth*, Biosystems, **91** (2008), 268–288. 1
- [6] M. Caputo, M. Fabrizio, A new definition of fractional derivative without singular kernel, Prog. Fract. Differ. Appl., 1 (2015), 73–85. 2.1, 3.1
- [7] L. G. de pillis, A. E. Radunskaya, C. L. Wiseman, A validated mathematical model of cell-mediated immune response to tumor growth, Cancer Res., 65 (2005), 7950–7958. 3
- [8] K. Diethelm, N. J. Ford, A. D. Freed, A predictor-corrector approach for the numerical solution of fractional differential equations, Nonlinear Dyn., 29 (2002), 3–22. 7
- [9] S. Esmaili, F. Nasresfahani, M. R. Eslahchi, Solving a fractional parabolic-hyperbolic free boundary problem which models the growth of tumor with drug application using finite difference-spectral method, Chaos Solitons Fractals, 132 (2020), 17 pages. 1
- [10] M. F. Farayola, S. Shafie, F. M. Siam, I. Khan, Mathematical modeling of radiotherapy cancer treatment using caputo fractional derivative, Comput. Methods Programs Biomed., 188 (2020), 39 pages. 1
- [11] L. Galluzzi, E. Morselli, O. Kepp, I. Vitale, A. Rigoni, E. Vacchelli, M. Michaud, H. Zischka, M. Castedo, G. Kroemer, *Mitochondrial gateways to cancer*, Mol. Asp. Med., **31** (2010), 1–20. 1
- [12] P. T. Hamilton, B. R. Anholt, B. H. Nelson, Tumour immunotherapy: lessons from predator-prey theory, Nat. Rev. Immunol., 22 (2022), 765–775. 1
- [13] D. Hanahan, R. A. Weinberg., The hallmarks of cancer, Cell, 100 (2000), 57–70. 1
- [14] M. Idrees, A. S. Alnahdi, M. B. Jeelani, Mathematical modeling of breast cancer based on the Caputo-Fabrizio fractal-fractional derivative, Fractal Fract., 7 (2023), 14 pages. 3
- [15] G. Jordão, J. N. Tavares, Mathematical models in cancer therapy, Biosystems, 162 (2017), 12–23. 1
- [16] I. Kareva, K. Luddy, C. O'Farrelly, R. Gatenby, J. Brown, *Predator-prey in tumor-immune interactions: A wrong model or just an incomplete one?*, Front. Immunol., **12** (2021), 14 pages. 1
- [17] G. Kaur, N. Ahmad, On study of immune response to tumor cells in prey-predator system, Int. Sch. Res. Not., 2014 (2014), 8 pages. 1, 3, 5, 7
- [18] S. Khajanchi, J. J. Nieto, *Mathematical modeling of tumor-immune competitive system, considering the role of time delay*, Appl. Math. Comput., **340** (2019), 180–205. 1
- [19] V. Koudelakova, M. Kneblova, R. Trojanec, J. Drabek, M. Hajduch, Non-small cell lung cancer–genetic predictors, Biomed. Pap. Med. Fac. Univ. Palacky Olomouc Czech Repub., 157 (2013), 125–136. 1
- [20] V. A. Kuznetsov, I. A. Makalkin, M. A. Taylor, A. S. Perelson, Nonlinear dynamics of immunogenic tumors: Parameter estimation and global bifurcation analysis, Bull. Math. Biol., 56 (1994), 295–321. 3
- [21] H.-L. Li, L. Zhang, C. Hu, Y.-L. Jiang, Z. Teng, Dynamical analysis of a fractional-order predator-prey model incorporating a prey refuge, J. Appl. Math. Comput., 54 (2017), 435–449. 2.5
- [22] J. Losada, J. J. Nieto, *Properties of a new fractional derivative without singular kernel*, Prog. Fract. Differ. Appl., **1** (2015), 87–92. 2.1, 2.2, 2.3
- [23] K. J. Mahasa, R. Ouifki, A. Eladdadi, L. de Pillis, *Mathematical model of tumor–immune surveillance*, J. Theoret. Biol., 404 (2016), 312–330. 1
- [24] G. E. Mahlbacher, K. C. Reihmer, H. B. Frieboes, *Mathematical modeling of tumor-immune cell interactions*, J. Theoret. Biol., **469** (2019), 47–60. 1
- [25] G. Mani, A. J. Gnanaprakasam, S. Ramalingam, A. S. A. Omer, I. Khan, Mathematical model of the lumpy skin disease using Caputo fractional-order derivative via invariant point technique, Sci. Rep., 15 (2025), 16 pages. 1
- [26] I. Podlubny, Fractional differential equations, Academic Press, San Diego, CA, (1999). 2.1, 2.4
- [27] R. N. Premakumari, C. Baishya, M. K. A. Kaabar, Dynamics of a fractional plankton-fish model under the influence of toxicity, refuge, and combine-harvesting efforts, J. Inequal. Appl., 2022 (2022), 26 pages. 1
- [28] R. Ramaswamy, G. Mani, R. Mohanraj, O. Ege, Mathematical SEIR model of the lumpy skin disease using Caputo-Fabrizio fractional-order, Eur. J. Pure Appl. Math., 18 (2025), 25 pages. 1
- [29] A. S. Rashed, M. M. Mahdy, S. M. Mabrouk, R. Salah, *Fractional order mathematical model for predicting and controlling Dengue fever spread based on awareness dynamics*, Computations, **13** (2025), 16 pages. 1
- [30] F. A. Rihan, M. Safan, M. A. Abdeen, D. Abdel Rahman, Qualitative and computational analysis of a mathematical model for tumor-immune interactions, J. Appl. Math., 2012 (2012), 19 pages. 1, 3
- [31] F. A. Rihan, G. Velmurugan, Dynamics of fractional-order delay differential model for tumor-immune system, Chaos Solitons Fractals, 132 (2020), 14 pages. 1
- [32] E. Y. Salah, B. Sontakke, A. A. Hamoud, H. Emadifar, A. Kumar, A fractal-fractional order modeling approach to understanding stem cell-chemotherapy combinations for cancer, Sci. Rep., 15 (2025), 16 pages. 1
- [33] R. D. Schreiber, L. J. Old, M. J. Smyth, Cancer immunoediting: Integrating immunity's roles in cancer suppression and promotion, Science, 331 (2011), 1565–1570. 1
- [34] R. L. Siegel, K. D. Miller, N. S. Wagle, A. Jemal, Cancer statistics 2023, CA Cancer J. Clin., 73 (2023), 17–48. 1
- [35] J. G. Silva, A. C. O. Ribeiro, R. F. Camargo, P. F. A. Mancera, F. L. P. Santos, *Stability analysis and numerical simulations via fractional calculus for tumor dormancy models*, Commun. Nonlinear Sci. Numer. Simul., **72** (2019), 528–543. 1
- [36] P. Veeresha, A numerical approach to the coupled atmospheric ocean model using a fractional operator, Math. Model.

- Numer. Simul. Appl., 1 (2021), 1-10. 1
- [37] M. D. Vesely, M. H. Kershaw, R. D. Schreiber, M. J. Smyth, *Natural innate and adaptive immunity to cancer*, Annu. Rev. Immunol., **29** (2011), 235–271. 1
- [38] M. Yavuz, N. Sene, Stability analysis and numerical computation of the fractional predator-prey model with the harvesting rate, Fractal Fract., 4 (2020), 22 pages. 1
- [39] Zakirullah, C. Lu, L. Li, K. Shah, B. Abdalla, T. Abdeljawad, *Mathematical insights into chaos in fractional-order fishery model*, Model. Earth Syst. Environ., **11** (2025), 17 pages. 1